The Kuramoto model on directed and signed graphs*

Robin Delabays [†‡] Philippe Jacquod [†] Florian Dörfler [‡]

July 30, 2018

Abstract

Many real-world systems of coupled agents exhibit directed interactions, meaning that the influence of an agent on another is not reciprocal. Furthermore, interactions usually do not have identical amplitude and/or sign. To describe synchronization phenomena in such systems, we use a generalized Kuramoto model with directed, weighted and signed interactions. Taking a bottom-up approach, we investigate the simplest possible directed networks, namely acyclic directed networks and directed cycles. These two types of networks are fundamental building blocks from which many general directed networks can be constructed. For acyclic, weighted and signed networks, we are able to completely characterize synchronization properties through necessary and sufficient conditions, which we show are optimal. Additionally, we prove that if it exists, a stable synchronous state is unique. In directed, weighted and signed cycles with identical natural frequencies, we show that the system globally synchronizes and that the number of stable synchronous states is finite.

Keywords. Kuramoto model, synchronization, directed graphs, acyclic graphs, directed cycles, weighted graphs, signed graphs.

AMS subject classifications. 34D06, 37N35

1 Introduction

Since its introduction in 1975 [1], the Kuramoto model has imposed itself as a standard mathematical model to describe the large variety of synchronization phenomena encountered in natural and human-made systems. References [2, 3, 4] give some extensive surveys about it. In its initial formulation, the Kuramoto model describes the time evolution of a group of n oscillators, each characterized by a natural frequency $\omega_i \in \mathbb{R}$, with identical and symmetric coupling $K/n > 0$,

$$\dot{\theta}_i = \omega_i - \frac{K}{n} \sum_{j=1}^{n} \sin(\theta_i - \theta_j) \,, \qquad i \in \{1, ..., n\} \,. \tag{1}$$

It has been shown [5, 6] that under the assumption that the distribution of natural frequencies has compact support, there exists a critical coupling strength, $K_c > 0$, such that the oscillators frequency-synchronize, meaning that for all $i, j \in \{1, ..., n\}$,

$$\lim_{t\to\infty} \dot{\theta}_i = \lim_{t\to\infty} \dot{\theta}_j \,, \tag{2}$$

if $K > K_c$.

The Kuramoto model achieves a good compromise between the simplicity of expression, allowing for an analytical approach, and the complexity of synchronization behaviors described. During the last decades, the interest in the Kuramoto model increased in many fields of science and engineering. It has been shown that it can be used to describe synchronization phenomena in domains as various as biology [7, 8, 9], physics [10, 11] and engineering [12].

*This work has been supported by ETH Zürich funding and the SNSF AP Energy grant PYAPP2_154275

†University of Applied Science of Western Switzerland, CH-1950 Sion, Switzerland, (robin.delabays@hevs.ch, philippe.jacquod@hevs.ch).

‡Automatic Control Laboratory, Swiss Federal Institute of Technology (ETH) Zürich, Switzerland, (dorfler@ethz.ch).

To better represent real-world systems, the Kuramoto model has been generalized in many different ways [12, 13]. One of the main generalizations, is to consider the Kuramoto model with interactions given by an arbitrary graph,

$$\dot{\theta}_i = \omega_i - \sum_{j=1}^{n} a_{ij} \sin(\theta_i - \theta_j)\,, \qquad\qquad i \in \{1, ..., n\}\,, \tag{3}$$

where a_{ij} is the $(i,j)^{\text{th}}$ element of the weighted adjacency matrix of the considered graph.

In the vast majority of the literature on the Kuramoto model, the interactions are considered symmetric and positive, i.e., $a_{ij} = a_{ji} > 0$. However, in some systems exhibiting synchronizing behaviors, the interaction can be nonsymmetric ($a_{ij} \neq a_{ji}$) or even unidirectional ($a_{ij} \neq 0 \implies a_{ji} = 0$) [14, 15, 16, 17]. Some systems also exhibit negative couplings, observed in particular in social networks, when some agents adjust their ideas in opposition to some others, and in interactions between neurons that can be excitatory ($a_{ij} > 0$) or inhibitory ($a_{ij} < 0$) [15, 16, 18, 19]. In this manuscript, we focus on the Kuramoto model with unidirectional interactions, which we refer to as *directed interactions*, and we consider general coupling weights, that can be positive or negative, referred to as *signed interactions*.

Investigations about the Kuramoto model with mixed positive and negative couplings showed that with all-to-all coupling, synchronization depends on the ratio between the number of positive and negative couplings [20, 21].

In [14], the authors give some estimation of the critical coupling K_c in the limit of large ($n \gg 0$) directed networks, as well as networks with mixed positive and negative couplings. Some conditions for the existence of frequency-synchronous state in general directed networks are given in [22], and [23] give some conditions for the existence of frequency-synchronous states in complete directed, weighted and signed networks. The authors of [24] show that in directed networks, synchronization is favored if the natural frequencies and the out-degrees (called *in-degrees* in their article) of the oscillators are correlated.

All previously cited references consider either all-to-all coupling or general interaction graphs, without restriction on the type of graphs considered. We choose here a bottom-up approach, starting with the simplest directed networks possible, i.e., directed acyclic networks and directed cycles. For weighted and signed directed acyclic networks, we give some explicit necessary and sufficient conditions for global synchronization of the system. For weighted and signed directed cycles, with identical natural frequencies, we prove global synchronization and show that the final synchronization frequency can take only discrete values.

The Kuramoto model on acyclic directed graphs has been investigated in [25], where the authors give some local subdomains of the state space where initial condition are guaranteed to lead to synchronization. In section 2, we completely characterize the synchronization properties of the Kuramoto model on weighted and signed directed acyclic graphs. We give some necessary and sufficient conditions on the system's parameters (edge weights and natural frequencies) for the existence of a globally exponentially stable synchronous state. Furthermore, this synchronous state is unique. We show by examples that our necessary and sufficient conditions cannot be sharpened in general. It is remarkable that our results hold regardless of the signs of the couplings in the network.

On directed cycles, Rogge and Aeyels [26] obtained an upper bound on the number of stable synchronous states of the Kuramoto model with cyclic directed interactions, for general natural frequency distribution. To the best of our knowledge, the best estimate of the region of synchronization for identical natural frequencies is given in [27], where the authors explicitly determine a subdomain of the state space where the system always synchronizes. They further identify subdomains of the basins of attraction of the various synchronous states. In section 3, we show that, in the case of identical natural frequencies, the system globally synchronizes, again regardless of the sign and magnitude of the couplings. We further prove that each stable synchronous state corresponds to a different synchronous frequency, and the the number of such synchronous frequencies is finite. We express them as solutions of an equation.

In section 4, we illustrate the difficulty to generalize our results to more complex interaction graphs. Using directed acyclic networks and directed cycles as building blocks, we construct more general directed graphs where we attempt to extend the results of the previous sections. We show that in some cases our results can be directly generalized, but we also identify some cases where the system synchronizes or not depending on the initial conditions of the oscillators. The Kuramoto dynamics reveal to be rather complex in general directed and signed networks.

1.1 Definitions and properties

We consider a generalized Kuramoto model with directed weighted, and real-valued (not necessarily positive) interactions

$$\dot{\theta}_i = \omega_i - \sum_{j=1}^{n} a_{ij} \sin(\theta_i - \theta_j)\,, \qquad\qquad i \in \{1, ..., n\}\,, \tag{4}$$

where $\theta_i \in \mathbb{S}^1 \simeq \mathbb{R}/(2\pi\mathbb{Z})$ and $\omega_i \in \mathbb{R}$ are the i^{th} oscillator's angle and natural frequency respectively, $a_{ij} \in \mathbb{R}$ is the coupling constant between oscillators i and j, and n is the number of oscillators. The coupling is a priori not symmetric, we allow negative edge weights, and $a_{ij} = 0$ means that there is no edge from i to j. The interaction graph is then directed, signed and weighted. The oscillators' angles are aggregated in the *state* $\boldsymbol{\theta} \in \mathbb{T}^n$. For any $c \in \mathbb{R}$ and $\boldsymbol{k} \in \mathbb{Z}^n$, the states $\boldsymbol{\theta}$ and $\boldsymbol{\theta} + 2\pi \cdot \boldsymbol{k} + c \cdot (1, ..., 1)$ are equivalent with respect to the dynamics of (4).

A *weighted, signed and directed graph* $\mathcal{G} = (\mathcal{V}, \mathcal{E}, A)$ is defined by a set of vertices $\mathcal{V} \coloneqq \{1, ..., n\}$, a set of edges $\mathcal{E} \subset \mathcal{V} \times \mathcal{V}$ which are ordered pairs of vertices, and a weighted adjacency matrix A, where $a_{ij} \neq 0$ if and only if the edge (i, j) from vertex i to vertex j belongs to $\mathcal{E}$. In this manuscript, we consider finite ($n < \infty$) unidirected graphs ($a_{ij} \neq 0 \implies a_{ji} = 0$) without self-loops ($a_{ii} = 0$). In a directed graph, if there exists an edge from vertex i to vertex j, we call i the *parent* of j, and j is the *child* of i. Vertices without children are called *leaders*, and the set of leaders is $\mathcal{L} \subset \mathcal{V}$. A *path* from vertex i to vertex j is a sequence of edges $\mathcal{P}_{ij} \coloneqq (\ell_1, ..., \ell_L)$, where i is the parent of edge ℓ_1, j is the child of edge ℓ_L, and for all $p = 1, ..., L$, ℓ_p is an edge of $\mathcal{G}$ and the parent of ℓ_{p+1} is the child of ℓ_p. A path is *simple* if it does not go twice through an edge. A *cycle* is a simple path from a vertex to itself. If a graph does not contain any cycle, it is *acyclic*.

1.2 Local order parameter

For the standard Kuramoto model, with undirected interactions given by (1), the *order parameter*,

$$re^{i\psi} \coloneqq \frac{1}{n} \sum_{j=1}^{n} e^{i\theta_j}\,, \tag{5}$$

gives a measure of alignment of the oscillators. In particular, the dynamics of each oscillator can be written with respect to the order parameter only [4]. Following the same idea, we define the *local order parameter* of vertex j (a similar definition was given in [14]),

$$r_j e^{i\psi_j} \coloneqq \sum_{k \neq j} a_{jk} e^{i\theta_k}\,, \tag{6}$$

which is equivalently rewritten in real and imaginary parts as

$$r_j \cos(\psi_j) = \sum_k a_{jk} \cos(\theta_k)\,, \qquad\qquad r_j \sin(\psi_j) = \sum_k a_{jk} \sin(\theta_k)\,, \tag{7}$$

with $\psi_j \in \mathbb{S}^1$ and $r_j \in \mathbb{R}_{\geq 0}$. The dynamics (4) of each oscillator can then be rewritten

$$\dot{\theta}_i = \omega_i - r_i \sin(\theta_i - \psi_i)\,, \qquad\qquad i \in \{1, ..., n\}\,, \tag{8}$$

where we recall that r_i and ψ_i depend on other angles. We define the *out-degree* of vertex j,

$$d_j^{\text{out}} \coloneqq \sum_{k=1}^{n} |a_{jk}|\,, \tag{9}$$

and indexing the children of j from 1 to n_j such that

$$|a_{j1}| \geq |a_{j2}| \geq \ldots \geq |a_{jn_j}|\,, \tag{10}$$

we define

$$\rho_j \coloneqq \max\left\{0, |a_{j1}| - \sum_{k=2}^{n_j} |a_{jk}|\right\}. \tag{11}$$

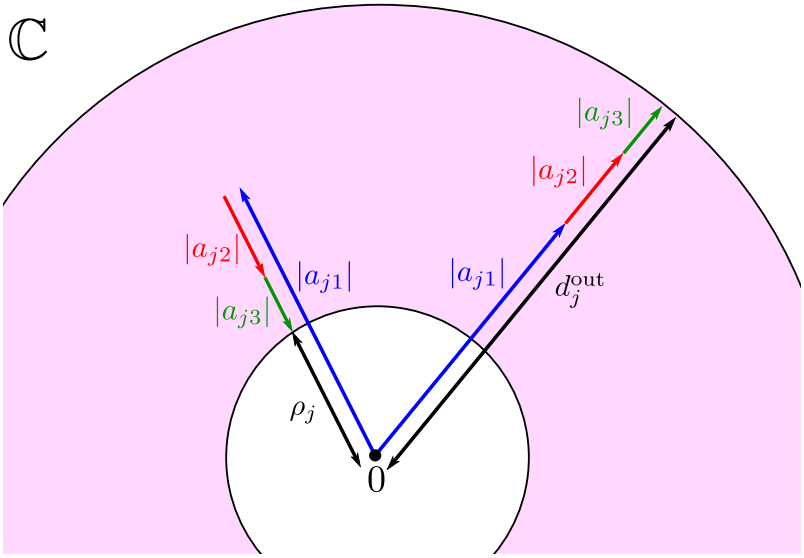

Figure 1: *The possible complex values of the local order parameter for a vertex with 3 children are in the pink area. The two extreme cases of smallest/largest order parameter amplitude are depicted. When all angles are aligned, the amplitude of the order parameter is d_j^{out} and when all angles are π appart from θ_1, the order parameter has amplitude ρ_j.*

Proposition 1.1. *For any directed, weighted and signed graph, the amplitude of the local order parameter r_j belongs to the interval $[\rho_j, d_j^{\text{out}}]$. Furthermore, we can construct angle distributions realizing both end values of this interval.*

Proof. The upper bound is a direct application of the triangle inequality,

$$r_j = \left| \sum_k a_{jk} e^{i\theta_k} \right| \leq \sum_k |a_{jk} e^{i\theta_k}| = \sum_k |a_{jk}| = d_j^{\text{out}} \,. \tag{12}$$

The amplitude of the local order parameter r_j is by definition larger or equal to zero, and the triangle inequality gives also

$$r_j = \left| \sum_k a_{jk} e^{i\theta_k} \right| \geq \left| a_{j1} e^{i\theta_1} \right| - \left| \sum_{k=2}^{n_j} a_{jk} e^{i\theta_k} \right| \geq |a_{j1}| - \sum_{k=2}^{n_j} |a_{jk}| \,. \tag{13}$$

By definition, ρ_j is then a lower bound for r_j. This proves the first part of the proposition.

We prove the second part for nonnegative weights. The argument can be easily adjusted in case some weights are negative. The value $r_j = \rho_j$ is realized when the angles θ_k, $k = 2, ..., n_j$ are all equal and π appart from θ_1: $\theta_2 = ... = \theta_{n_j} = \theta_1 \pm \pi$. When all these angles are identical, $\theta_1 = ... = \theta_{n_j}$, then $r_j = d_j^{\text{out}}$. Thus both ends of the interval can be reached for some angle distributions, both cases are illustrated in Figure 1. □

Remark 1.2. *In the particular case where j has a single out-going edge, then $\rho_j = d_j^{\text{out}} = r_j$. When j has two children, $\rho_j = |a_{j1}| - |a_{j2}|$, which is zero if and only if the weights have the same absolute value. In general, if j has three or more children, ρ_j will be zero if weights are not too different.*

1.3 Synchronization

If not specified otherwise, *synchronization* refers to frequency-synchronization, which means $\dot{\theta}_i = \dot{\theta}_j$ for all i, j. At a synchronous state of the directed Kuramoto model, all angles rotate at the same frequency and angle differences are constant in time. It is necessary for synchronization that all leaders have the same natural frequency, and that the deviation from leader frequency is bounded by the weighted out-degree.

Proposition 1.3. *Let $\mathcal{G}$ be a directed, weighted, and signed graph, with at least one leader. If the dynamical system (4) with interaction graph $\mathcal{G}$ has a synchronous state, then*

(i) the leaders have identical natural frequency $\omega_i = \omega_{\rm L}$ for all $i \in \mathcal{L}$; and
(ii) for all $i \in \{1, ..., n\}$,

$$|\omega_i - \omega_{\rm L}| \leq d_i^{\rm out} \,. \tag{14}$$

Proof. (i) By definition, at a synchronous state, all oscillators, and leaders in particular, have the same frequency $\dot{\theta}_i = \omega_{\rm L}$, $i \in \{1, ..., n\}$. By definition again, the dynamics of leaders, given by (4) reduce to

$$\dot{\theta}_i = \omega_i \,, \qquad\qquad i \in \mathcal{L} \,. \tag{15}$$

The leaders have then the same natural frequency, $\omega_i = \omega_{\rm L}$, $i \in \mathcal{L}$.

(ii) If $|\omega_i - \omega_{\rm L}| > d_i^{\rm out}$, according to Proposition 1.1, the right-hand-side of (8) is strictly larger than $\omega_{\rm L}$ in absolute value and the system is then not synchronous. This concludes the proof by contraposition. □

Without loss of generality, we can consider all angles in a frame rotating at a given frequency. Throughout this manuscript, if a network contains leaders and they have identical natural frequency $\omega_{\rm L}$, we apply the change of variable

$$\theta_i(t) \to \theta_i(t) - \omega_{\rm L} t \,. \tag{16}$$

After this, leaders have zero natural frequency and a synchronous state at the leader frequency is an equilibrium of (4), meaning that all frequencies are zero. We will see that other synchronous states can occur in cyclic interaction graphs

If for all initial conditions, the system (4) converges to a synchronous state, we say that it *globally synchronizes*. We say that a synchronous state is *almost globally stable* if almost all initial conditions converge to it. If furthermore convergence is exponential, the synchronous state is *almost globally exponentially stable*.

2 Directed acyclic networks

An acyclic directed graph contains at least one leader. Proposition 1.3 gives then necessary conditions for the existence of a synchronous state of (4), and in particular for global synchronization, on such a network. We give now a sufficient condition for global synchronization in such networks. We show then that the necessary and sufficient conditions we obtained cannot be improved. Finally, we show that there is a unique stable synchronous state in such networks.

2.1 Sufficient condition

We give a general sufficient condition guaranteeing the synchronization of the dynamical system. Our argument relies on a series of results from [28], which we recall in Appendix A for completeness.

Theorem 2.1. *Let us consider the dynamical system (4), where the interaction graph is directed, acyclic, weighted, and signed, and assume that*

$$|\omega_i| \leq \rho_i \,, \qquad\qquad i \in \{1, ..., n\} \,. \tag{17}$$

Then the system globally synchronizes.

Remark 2.2. *Equation* (17) *is always satisfied for the leaders where $\omega_i = \rho_i = 0$.*

Proof. We prove recursively that all oscillators converge to a steady state, i.e., $\dot{\theta}_i(t \to \infty) = 0$. Initial conditions (at time $t = 0$) are $\boldsymbol{\theta}^\circ \in \mathbb{T}^n$ and equilibrium towards which the system converges, if it exists, is $\boldsymbol{\theta}^* \in \mathbb{T}^n$. Note that all variable quantities in this proof depend on initial conditions, but we do not explicitly write this dependence for sake of readability.

Base case. According to (4), if i is a leader, $\dot{\theta}_i \equiv 0$, and it trivially converges to a steady state,

$$\lim_{t\to\infty} \theta_i = \theta_i^* = \theta_i^\circ \,. \tag{18}$$

Induction step. Assume that all children j of i converge to a steady state, $\lim_{t\to\infty} \dot{\theta}_j = 0$ and $\lim_{t\to\infty} \theta_j = \theta_j^*$. Let us prove that i converges to a steady state as well, $\lim_{t\to\infty} \theta_i = \theta_i^*$.

Using the local order parameter, we can write (4) as the nonautonomous system

$$\dot{\theta}_i = \omega_i - r_i(t)\sin\left[\theta_i - \psi_i(t)\right] =: f(t,\theta_i)\,, \tag{19}$$

where we write r_i and ψ_i as time-dependent variables because for a given initial state of the system $\boldsymbol{\theta}^\circ$, from the point of view of the i^{th} oscillator, these values depend only on time. Children are not influenced by parents, due to the acyclic topology of the graph. The solution θ_i can be seen as a nonautonomous semiflow (Definition A.1) for (19). As all children of i converge to a fixed angle, there exists $r_i^* \in [\rho_i, d_i^{\text{out}}]$ and $\psi_i^* \in \mathbb{S}^1$ such that

$$\lim_{t\to\infty} r_i(t) = r_i^*\,, \qquad\qquad \lim_{t\to\infty} \psi_i(t) = \psi_i^*\,. \tag{20}$$

We also define the autonomous system

$$\dot{\varphi}_i = \omega_i - r_i^*\sin\left[\varphi_i - \psi_i^*\right] =: g(\varphi_i)\,, \tag{21}$$

with initial conditions $\boldsymbol{\varphi}(0) = \boldsymbol{\theta}^\circ$. The solution φ_i of (21) is an autonomous semiflow (Definition A.1). Observe that (21) equals the time-varying dynamics (19) only if $\psi_i(t)$ and $r_i(t)$ have converged to their steady-state value. We show now that the dynamical systems (19) and (21) with the same initial conditions, always converge to the same set of fixed points.

The *ω-limit set* of θ_i is

$$\Lambda_i(\boldsymbol{\theta}^\circ) \coloneqq \left\{\theta \in \mathbb{S}^1 \colon \exists\, \{t_j\},\ j\in\mathbb{N},\ \text{s.t. } \lim_{j\to\infty} t_j = \infty \text{ and } \lim_{j\to\infty} \theta_i(t_j) = \theta\right\}\,, \tag{22}$$

which is the domain towards which θ_i converges under the dynamics of (19), as $t\to\infty$.

The functions $f(t,\cdot)$ and $g(\cdot)$ are bounded, continuous and 2π-periodic on $\mathbb{R}$. They are then naturally defined on the compact quotient space $\mathbb{S}^1$, which we parametrize by angles in $(-\pi,\pi]$. Furthermore, as $t\to\infty$, f converges to g. It is then a standard result of analysis that convergence of a function defined on a compact set is uniform.* In particular $f(t,\cdot)\to g(\cdot)$ uniformly on any compact subset of $\mathbb{S}^1$, as $t\to\infty$. Proposition A.2 then implies that θ_i is asymptotically autonomous with limit semiflow φ_i (Definition A.1). Theorem A.3 implies first that θ_i converges to Λ_i and second that Λ_i is invariant for φ_i, which tells us that

$$\varnothing \neq \Lambda_i \subset \mathcal{I}_i\,, \tag{23}$$

where $\mathcal{I}_i$ is the invariant set of (21).

By Proposition 1.1, $r_i^* \geq 0$. If $r_i^* > 0$, the invariant set of the dynamics (21) is composed of two points,

$$\mathcal{I}_i \coloneqq \{\arcsin(\omega_i/r_i^*) + \psi_i^*, \pi - \arcsin(\omega_i/r_i^*) + \psi_i^*\}\,, \tag{24}$$

which are well-defined by hypothesis (17). The ω-limit set Λ_i is then discrete and θ_i converges to a single point $\theta_i^* \in \Lambda_i \subset \mathcal{I}_i$. As both points of $\mathcal{I}_i$ cancel the right-hand-side of (21), $\lim_{t\to\infty}\dot{\theta}_i = 0$.

If $r_i^* = 0$, then by assumption, $\omega_i = 0$. The right-hand-side of (21) is then zero for all time and the right-hand-side of (19) goes to zero as $t\to\infty$. The invariant set of the dynamics (21) is then $\mathcal{I}_i = \mathbb{S}^1$, and

$$\varnothing \neq \Lambda_i \subset \mathbb{S}^1\,. \tag{25}$$

It implies $\lim_{t\to\infty}\dot{\theta}_i = 0$ and θ_i converges to some fixed $\theta_i^* \in \mathbb{S}^1$. This concludes the proof of the induction step.

According to the base case, the leaders are synchronized. Applying then the induction step implies that the leaders' parents synchronize with the leaders. As there is a finite number of oscillators, a recursive application of the induction step implies synchronization of all oscillators with the leaders, which completes the proof. □

If an oscillator i has a single child j, then $\rho_i = d_i^{\text{out}} = |a_{ij}|$ and, by Theorem 2.1 and Proposition 1.3, equation (17) for vertex i is a necessary and sufficient condition for global synchronization.

Corollary 2.3. *If all vertices have at most one out-going edge, then the system globally synchronizes if and only if for all nonleader oscillators, $|\omega_i| \leq |a_{ij}|$, where j is i's child.*

The case of identical natural frequencies ($\omega_i \equiv 0$) is a particular case of Theorem 2.1.

Corollary 2.4. *Consider the dynamical system (4) with identical natural frequencies ($\omega_i \equiv 0$) where the interaction graph is directed, acyclic, weighted, and signed. Then the system globally synchronizes.*

*Here *uniform* means that $\forall\ \varepsilon > 0$, $\exists\ T > 0$ such that $|f(t,\theta) - g(\theta)| < \varepsilon$, $\forall\ t \geq T$ and $\forall\ \theta \in \mathbb{S}^1$.

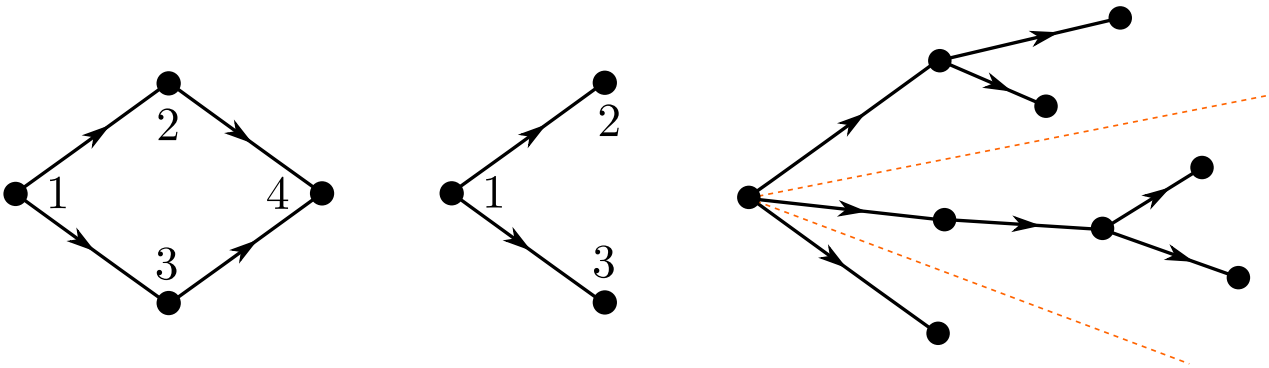

Figure 2: *Left: Example of an acyclic network where there exists* $\delta > 0$ *such that* $\rho_1 + \delta < r_1^* < d_1^{\text{out}} - \delta$*, for any initial conditions. Network parameters are* $(\omega_1, \omega_2, \omega_3, \omega_4) = (0, \sqrt{3}, -2, 0)$ *and* $(a_{12}, a_{13}, a_{24}, a_{34}) = (1, \sqrt{3}, 2, 4)$*. This gives* $\rho_1 = \sqrt{3}-1$ *and* $d_1^{\text{out}} = \sqrt{3}+1$*, while* $r_1^* \in \{1, 2\}$*. Center: Example of an acyclic network where, depending on initial conditions,* r_1^* *can take any value in the interval* $[\rho_i, d_i^{\text{out}}]$*. Network parameters are* $\omega_1 = \omega_2 = \omega_3 = 0$ *and* $(a_{12}, a_{13}) = (1, 2)$*. This gives* $\rho_1 = 1$ *and* $d_1^{\text{out}} = 3$*. Right: Example of a directed graph where the edges going out of a vertex belong to independent subgraphs. In this case, depending on initial conditions, the local order parameter can take any value in* $[\rho_i, d_i^{\text{out}}]$*.*

2.2 Tightness of the conditions

We now give examples of two simple acyclic graphs to illustrate how tight our necessary and sufficient conditions (14) and (17) are. The amplitude of the local order parameter r_i^* depends only on the initial conditions of the leaders $\boldsymbol{\theta}^\circ$, and we know that

$$\min_{\boldsymbol{\theta}^\circ} r_i^* \geq \rho_i \,. \tag{26}$$

Depending on the graph topology, the inequality (26) can be tight or not.

Example 2.5. *Consider the network in the center panel of Figure 2, where* $\rho_1 = 1$ *and* $d_1^{\text{out}} = 3$*. Consider initial conditions such that* $\theta_2^\circ - \theta_3^\circ = \phi$*. For* $\phi = 0$*, we obtained* $r_1^* = d_1^{\text{out}} = 3$ *and for* $\phi = \pi$ *we have* $r_1^* = \rho_1$*. Both bounds* (17) *and* (14) *are reached for some initial condition and while* ϕ *is ranging from* 0 *to* π*, all values of the interval* $[\rho_1, d_1^{\text{out}}]$ *are obtained.*

This example satisfies the hypothesis of Corollaries 2.3 and 2.4. Both bounds are tight and valid depending on initial conditions, i.e., our bounds are as good as they get. For some networks, the sufficient condition of Theorem 2.1 is as well necessary for global synchronization. It also means that for these networks, equation (14) is a sufficient condition for the existence of an equilibrium.

Example 2.6. *Consider the network in the left panel of Figure 2, where* $\rho_1 = \sqrt{3}-1$ *and* $d_1^{\text{out}} = \sqrt{3}+1$*. According to Theorem 2.1, the system globally synchronizes for* $\omega_1 \leq \rho_1$*. We can compute that for all initial conditions, either* $r_1^* = 1$ *or* $r_1^* = 2$*. Then, the system also globally synchronizes for* $\rho_1 \leq \omega_1 < 1$*.*

In this example, the bounds are loose: synchronization is global for some natural frequencies violating (17); and impossible for some natural frequencies violating (14). The system globally synchronizes for $\rho_1 < \omega_1 \leq \min_{\boldsymbol{\theta}^\circ} r_1^*$.

Generally, the bounds (14) and (17) are tight if each edge going out of i is connected to an independent subgraph (right panel of Figure 2). Otherwise, the range of the local order parameter r_i^* is strictly smaller than the interval $[\rho_i, d_i^{\text{out}}]$.

2.3 Stability

We assess local stability of a synchronous state by linearizing the time evolution of a small perturbation of the angles. In the dynamical system (4) on an acyclic directed graph, fixed points depend on the initial conditions of the leaders. Perturbing the leaders then changes the fixed point, and the analysis is not relevant for the fixed point initially considered. To avoid this, we retrict our stability analysis to the dynamics where the leaders are fixed,

$$\dot{\theta}_i = \omega_i - \sum_{j=1}^{n} a_{ij} \sin(\theta_i - \theta_j) \,, \qquad\qquad i \in \mathcal{V} \setminus \mathcal{L} \,, \tag{27}$$

with $\theta_i(0) = \theta_i^\circ$, for $i \in \mathcal{V}$.

Theorem 2.7. *Consider the dynamical system (27), where the interaction graph is directed, acyclic, weighted and signed, and natural frequencies satisfy (17). A synchronous state $\boldsymbol{\theta}^*$ is almost globally exponentially stable if and only if*

$$\sum_{j=1}^{n} a_{ij} \cos(\theta_i^* - \theta_j^*) > 0\,, \qquad\qquad i \in \mathcal{V} \setminus \mathcal{L}\,. \tag{28}$$

In particular it is the unique stable synchronous state with $\theta_i = \theta_i^*$ for $i \in \mathcal{L}$.

Proof. In acyclic directed networks, the Jacobian matrix of the system (4) is lower triangular (up to renumbering the vertices), and its eigenvalues are its diagonal elements $\mathcal{J}_{ii} = -\sum_j a_{ij} \cos(\theta_i^* - \theta_j^*)$. An equilibrium is then linearly stable if and only if $\mathcal{J}_{ii} < 0$ for all $i \in \mathcal{V} \setminus \mathcal{L}$.

The *only if* direction is straightforward. Assume that $\boldsymbol{\theta}^*$ is almost globally exponentially stable. In particular it is locally exponentially stable and satisfies (28).

The *if* direction is more involved. Assume that the fixed point $\boldsymbol{\theta}^*$ satisfies (28). We first show that it is unique. The diagonal terms of the Jacobian can be rewritten with respect to the local order parameter,

$$\mathcal{J}_{ii} = -r_i \cos(\theta_i - \psi_i)\,, \qquad\qquad i \in \mathcal{V} \setminus \mathcal{L}\,. \tag{29}$$

If $\mathcal{J}_{ii} < 0$ for all $i \in \mathcal{V} \setminus \mathcal{L}$, then in particular, $r_i > 0$. According to the proof of Theorem 2.1, knowing the angles of the children of oscillator i, there are two possible values of θ_i at a fixed point: $\arcsin(\omega_i/r_i) + \psi_i$ and $\pi - \arcsin(\omega_i/r_i) + \psi_i$. Only the first one satisfies $\mathcal{J}_{ii} < 0$. There is then a unique fixed point satisfying (28), that we can construct recursively. This proves the last part of the theorem.

We now need to show that almost all initial conditions converge to $\boldsymbol{\theta}^*$. Assume that $\boldsymbol{\theta}^\dagger$ is a fixed point of (27) such that $\mathcal{J}_{ii} \geq 0$ for some $i \in \mathcal{V} \setminus \mathcal{L}$. Then $\boldsymbol{\theta}^\dagger \neq \boldsymbol{\theta}^*$, meaning that in the recursive construction of the fixed point described above, for some $j \in \mathcal{V} \setminus \mathcal{L}$ with $r_j > 0$, we chose $\theta_j^\dagger = \pi - \arcsin(\omega_j/r_j) + \psi_j$. Otherwise we would have constructed $\boldsymbol{\theta}^*$. But then

$$\mathcal{J}_{jj}(\boldsymbol{\theta}^\dagger) = -r_j \cos(\theta_j^\dagger - \psi_j) = r_j \cos(\theta_j^* - \psi_j) = -\mathcal{J}_{jj}(\boldsymbol{\theta}^*) > 0\,. \tag{30}$$

Then the fixed point $\boldsymbol{\theta}^\dagger$ has at least one unstable direction, and its region of attraction (set of states converging to it) is a submanifold of $\mathbb{T}^n$ of dimension at most $n-1$. It has then zero measure [29].

According to Theorem 2.1, the system globally converges to a fixed point, and the only one with nonzero measure region of attraction is $\boldsymbol{\theta}^*$. It is then almost globally stable. Finally, as it is locally exponentially stable, it is almost globally exponentially stable [30]. □

In the particular case of identical natural frequencies, the system reaches phase-synchronization, i.e., $\theta_i = \theta_j$ for all i, j.

Corollary 2.8. *Let us consider the dynamical system (4) with identical natural frequencies ($\omega_i \equiv 0$), where the interaction graph is directed, acyclic, weighted and signed. Then the phase-synchronous state is almost globally exponentially stable.*

Proof. The phase-synchronous state, $\theta_i = \theta_j$ for all i, j, is an equilibrium of the system given by (4), which satisfies the stability condition (28). By Proposition 2.7, it is almost globally exponentially stable. □

Remark 2.9. *We stress out that all results obtained in this section apply to any magnitude and sign of the coupling strengths. Our results can hardly be more general.*

3 Directed cycles with identical frequencies

Throughout section 2, we completely characterized synchronization in directed acyclic networks. We turn now to the simplest cyclic directed graph, namely the directed cycle. In this case, we are able to prove global synchronization for identical natural frequencies. Again, all the following results hold for any nonzero coupling constants.

We consider directed cycles of length n, as in Figure 3, with arbitrary edge weights. By appropriately indexing all vertices, equation (4) is then

$$\dot{\theta}_i = \omega_i - a_{i,i+1} \sin(\theta_i - \theta_{i+1})\,, \qquad\qquad i \in \{1, ..., n\}\,, \tag{31}$$

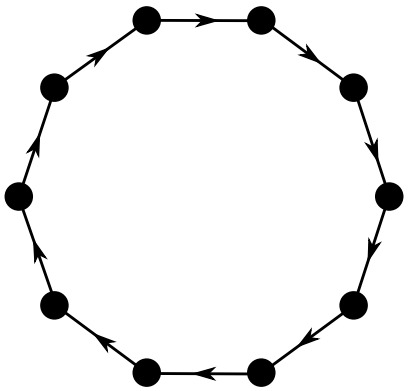

Figure 3: *Directed cycle of length $n = 10$. In section 3, we show global synchronization for these graphs.*

where indices are taken modulo n, and $a_{i,i+1} \in \mathbb{R}^*$.

With identical natural frequencies, directed cycles are very similar to undirected cycles. At a synchronous state, both cases admit the same angle differences (center panels of Figure 4). The difference being that in the undirected cycle, the oscillators synchronize to the mean natural frequency [4, sect. 3.1], which is zero (top right panel of Figure 4). At a synchronous state, angles are then constant (top left panel of Figure 4), i.e., a synchronous state is an equilibrium. In a directed cycle, the *synchronization frequency*, which is the frequency of all oscillators at a synchronous state and is denoted by ω_s, depends on the synchronous state (bottom right panel of Figure 4). In this case, oscillators rotate at the same, nonzero, frequency (bottom left panel of Figure 4). Stability of synchronous states is similar in directed [26] and undirected [31] cycles.

We will use the following short-hand notations:

$$s_i \coloneqq \sin(\theta_i) \qquad c_i \coloneqq \cos(\theta_i) \qquad s_{ij} \coloneqq \sin(\theta_i - \theta_j) \qquad c_{ij} \coloneqq \cos(\theta_i - \theta_j)\,, \tag{32}$$

and Δ_{ij} denotes the angle difference $\theta_i - \theta_j$ taken modulo 2π in the interval $(-\pi, \pi]$.

3.1 Global synchronization

In the case of identical frequencies ($\omega_i \equiv 0$), we are able to show global synchronization.

Theorem 3.1. *Consider the dynamical system (31) with identical natural frequencies. This dynamical system globally converges to a synchronous state.*

Proof. The function

$$\begin{aligned} V\colon \mathbb{T}^n &\longrightarrow \mathbb{R} \\ \boldsymbol{\theta} &\longmapsto 2 \cdot \sum_{i,j} a_{ij} \left[1 - \cos(\theta_i - \theta_j)\right]\,, \end{aligned} \tag{33}$$

is a LaSalle function [32] for the system under consideration. The function V is bounded, and its time derivative is given by

$$\dot{V} = -2 \cdot \sum_{i=1}^{n} a_{i,i+1}^2 s_{i,i+1}^2 - a_{i-1,i} a_{i,i+1} s_{i-1,1} s_{i,i+1} \tag{34}$$

$$= -\sum_{i=1}^{n} \left(a_{i-1,i} s_{i-1,i} - a_{i,i+1} s_{i,i+1}\right)^2 = -\sum_{i=1}^{n} \left(\dot{\theta}_{i-1} - \dot{\theta}_i\right)^2 \leq 0\,. \tag{35}$$

The system being defined on a compact manifold $\mathbb{T}^n$, LaSalle's invariance principle [32] implies that it converges to a synchronous state, because V is lower bounded and decreasing, and its time derivative vanishes only at synchronous states. □

The frequency of the oscillators at a synchronous state is bounded by the smallest coupling,

$$a_{\min} \coloneqq \min_i |a_{i,i+1}|\,. \tag{36}$$

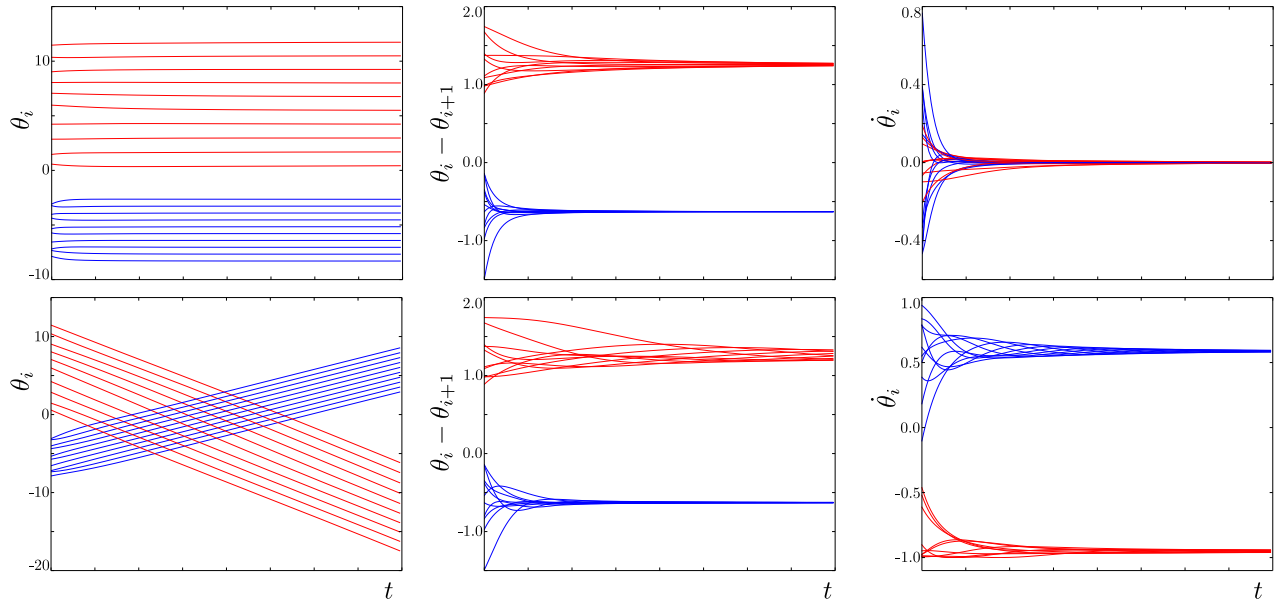

Figure 4: *Time evolution of angles (left), angle differences (center) and frequencies (right) according to the Kuramoto dynamics (4) with undirected (top) and directed (bottom) cyclic interactions. The cycle is of length $n = 10$ with identical natural frequencies and identical couplings. Blue and red lines correspond to two different initial conditions, leading to two different synchronous states. In the undirected case, angles converge to a fixed value (top left panel), which is not the case in the directed case (bottom left). Angle differences converge to the same value in both undirected and directed cycles (top and bottom center panels). At the synchronous state, the frequencies are always zero in the undirected cycle (top right panel), and possibly nonzero and different in the directed case (bottom right panel).*

Proposition 3.2. *The synchronization frequency ω_{s} belongs to the interval $[-a_{\min}, a_{\min}]$.*

Proof. The frequency ω_{s} has to satisfy

$$\omega_{\mathrm{s}} = -a_{i,i+1} s_{i,i+1} \,, \tag{37}$$

for all $i \in \{1, ..., n\}$, which implies

$$\omega_{\mathrm{s}} \in \bigcap_i [-|a_{i,i+1}|, |a_{i,i+1}|] = [-a_{\min}, a_{\min}] \,. \tag{38}$$

□

Remark 3.3. *In general the set of synchronization frequencies can be continuous. We present here an example inspired from [33, sect. VI]. Consider a directed cycle whose length n is a multiple of 4, with identical positive edge weights. Then the state $\boldsymbol{\theta}^\alpha \in \mathbb{T}^n$, defined by*

$$\theta_i^\alpha := \begin{cases} -(i-1)\pi/2 \,, & \text{if } i \text{ is odd,} \\ -(i-2)\pi/2 - \alpha \,, & \text{if } i \text{ is even,} \end{cases} \tag{39}$$

with $\alpha \in (0, \pi/2)$, has angle differences

$$\Delta_{i,i+1}^\alpha = \begin{cases} \alpha \,, & \text{if } i \text{ is odd,} \\ \pi - \alpha \,, & \text{if } i \text{ is even.} \end{cases} \tag{40}$$

It is then an unstable synchronous state of (31), regardless of the value of α. The continuum of values of α implies a continuum of synchronous states.

Restricting ourselves to stable synchronous states, we show below that their number is discrete.

3.2 Stability

A full stability analysis of the identical frequency case has been done in [26] for positive edge weights. We extend it to general nonzero edge weights.

Lemma 3.4. *A synchronous state $\boldsymbol{\theta}^*$ of (31) with identical natural frequencies is locally exponentially stable if and only if*

$$a_{i,i+1}\cos(\theta_i^* - \theta_{i+1}^*) > 0\,, \qquad\qquad i \in \{1,...,n\}\,. \tag{41}$$

Furthermore, at such a synchronous state with frequency ω_s, the angle differences are given by

$$\Delta_{i,i+1}^{\omega_\mathrm{s}} = \begin{cases} -\arcsin(\omega_\mathrm{s}/a_{i,i+1})\,, & \text{if } a_{i,i+1} > 0\,, \\ \pi + \arcsin(\omega_\mathrm{s}/a_{i,i+1})\,, & \text{if } a_{i,i+1} < 0\,, \end{cases} \qquad\qquad i \in \{1,...,n\}\,. \tag{42}$$

Proof. A synchronous state is locally exponentially stable if and only if the Jacobian matrix

$$\mathcal{J}(\boldsymbol{\theta}) = \begin{pmatrix} -a_{12}c_{12} & a_{12}c_{12} & & & & \\ & -a_{23}c_{23} & a_{23}c_{23} & & & \\ & & \ddots & \ddots & & \\ & & & \ddots & a_{n-1,n}c_{n-1,n} & \\ a_{n,1}c_{n,1} & & & & -a_{n,1}c_{n,1} \end{pmatrix}, \tag{43}$$

is Hurwitz. Due to invariance under rotation of all angles, at least one eigenvalue is zero, but this has no influence on the stability of the synchronous state. According to Gershgorin's Circle Theorem [34], the eigenvalues of $\mathcal{J}$ are nonpositive if and only if

$$a_{i,i+1}\cos(\theta_i^* - \theta_{i+1}^*) \geq 0\,, \qquad\qquad i \in \{1,...,n\}\,. \tag{44}$$

If $\cos(\theta_i^* - \theta_{i+1}^*) = 0$ for some $i \in \{1,...,n\}$, then the first-order term in the Taylor series of $\dot{\theta}_i$ is zero. As the second-order term is nonzero, according to the discussion in [35, sect. 1.2], the synchronous state is unstable. We conclude that a synchronous state is locally asymptotically stable if and only if

$$a_{i,i+1}\cos(\theta_i^* - \theta_{i+1}^*) > 0\,, \qquad\qquad i \in \{1,...,n\}\,. \tag{45}$$

As in this case the Jacobian is Hurwitz, $\boldsymbol{\theta}^*$ is locally exponentially stable, which proves the first part of the proposition.

For a synchronous state to be stable, the cosine of the angle difference $c_{i,i+1}$ must have the same sign as its edge weight $a_{i,i+1}$. We see that

$$\cos[-\arcsin(\omega_\mathrm{s}/a_{i,i+1})] \geq 0\,, \qquad\qquad \cos[\pi + \arcsin(\omega_\mathrm{s}/a_{i,i+1})] \leq 0\,, \tag{46}$$

where ω_s is the synchronization frequency, and conclude that the angle differences in a stable synchronous are given by (42). This concludes the proof. □

Remark 3.5. *All synchronous states are parametrized similarly as in* (42)*, not only the stable ones. At a synchronous state, the angle differences satisfy*

$$\Delta_{i,i+1}^{\omega_\mathrm{s}} \in \{-\arcsin(\omega_\mathrm{s}/a_{i,i+1}), \pi + \arcsin(\omega_\mathrm{s}/a_{i,i+1})\}\,. \tag{47}$$

3.3 Stable synchronization frequencies

We now characterize the possible synchronization frequencies corresponding to stable synchronous states, which we call *stable synchronization frequencies*. We define n^- to be the number of edges with negative weight and

$$\sigma \coloneqq \frac{1}{2\pi}\sum_{i=1}^{n} \arcsin\left(a_\mathrm{min}/|a_{i,i+1}|\right)\,. \tag{48}$$

Proposition 3.6. *Consider the dynamical system (31) with identical natural frequencies. The number of possible stable synchronization frequencies is discrete and is given by the number of integers in the interval* $(n^-/2-\sigma, n^-/2+\sigma)$*. In particular, for each stable synchronization frequency* ω_s*, there exist an integer* $q \in (n^-/2-\sigma, n^-/2+\sigma) \cap \mathbb{Z}$ *such that* ω_s *solves*

$$\sum_{i=1}^{n} \arcsin\left(\omega_s/|a_{i,i+1}|\right) = (n^- - 2q)\pi\,. \tag{49}$$

Proof. Let $\omega_s \in \mathbb{R}$ be the frequency at the stable synchronous state $\boldsymbol{\theta}^{\omega_s} \in \mathbb{T}^n$, and let us define $\mathcal{V}^+$ (resp. $\mathcal{V}^-$) the set of vertices whose out-going edge has positive (resp. negative) weight.

Following the stability analysis of section 3.2, the angle differences of the stable fixed point are given by (42). Furthermore, the sum of angle differences around the cycle has to be an integer multiple of 2π, called the *winding number* $q \in \mathbb{Z}$,

$$\sum_{i=1}^{n} \Delta_{i,i+1}^{\omega_s} = 2\pi q\,. \tag{50}$$

As angle differences are taken in $(-\pi, \pi]$, the winding number is bounded as $-n/2 \le q \le n/2$. Replacing (42) in (50) gives

$$-\sum_{i\in\mathcal{V}^+} \arcsin(\omega_s/a_{i,i+1}) + \sum_{i\in\mathcal{V}^-} \pi + \arcsin(\omega_s/a_{i,i+1}) = 2\pi q \tag{51}$$

$$-\sum_{i=1}^{n} \arcsin(\omega_s/|a_{i,i+1}|) = 2\pi q - \pi n^-\,, \tag{52}$$

which is (49).

The left-hand-side of (52) is monotonically decreasing in ω_s. For a given winding number q, there is then at most one value of ω_s satisfying (52). As the number of possible values for q is finite, the number of possible synchronization frequencies is finite as well.

By boundedness of ω_s (Proposition 3.2) and monotonicity of (52), we can compute the number of possible winding numbers, which is the number of possible stable synchronization frequencies. The lower bound $q_{\min}$ (resp. upper bound $q_{\max}$) is obtained by taking $\omega_s = a_{\min}$ (resp. $\omega_s = -a_{\min}$),

$$q_{\min} = \frac{n^-}{2} - \frac{1}{2\pi}\sum_{i=1}^{n} \arcsin\left(a_{\min}/|a_{i,i+1}|\right)\,, \qquad q_{\max} = \frac{n^-}{2} + \frac{1}{2\pi}\sum_{i=1}^{n} \arcsin\left(a_{\min}/|a_{i,i+1}|\right)\,. \tag{53}$$

When $\omega_s = \pm a_{\min}$, for each edge such that $a_{i,i+1} = \pm a_{\min}$, the angle difference is $\pm\pi/2$. Hence the corresponding term in the Jacobian matrix vanishes, and according to Lemma 3.4, the corresponding fixed point is unstable. Stable fixed points then cannot realize the extreme values of winding number $q_{\min}$ and $q_{\max}$ and the winding number belongs to the interval $(n^-/2-\sigma, n^-/2+\sigma)$. □

We can even construct the stable synchronous states. Let $q \in (n^-/2-\sigma, n^-/2+\sigma) \cap \mathbb{Z}$ and assume that ω_s solves (49). The corresponding stable synchronous state can be constructed by defining $\boldsymbol{\theta}^{\omega_s}$ as

$$\theta_i^{\omega_s} = -n_i^- + \sum_{j=1}^{i-1} \arcsin\left(\omega_s/|a_{j,j+1}|\right)\,, \qquad i \in \{1, ..., n\}\,, \tag{54}$$

where n_i^- is the number of edges with negative weight on the path from vertex 1 to vertex i. Furthermore this synchronous state is stable because by construction it satifies (41).

Proposition 3.6 implies that there is a finite number of stable synchronous states and completely characterizes them. In particular, it allows to compute the number of stable synchronous states for identical positive weights and identical frequencies, which was obtained by Rogge and Aeyels [26].

Corollary 3.7 (Rogge and Aeyels [26])**.** *For a directed cycle with identical positive weights and identical frequencies, the number of stable synchronous states is* $\mathcal{N} = 2 \cdot \mathrm{Int}\left[(n-1)/4\right] + 1$.

Proof. Identical positive weights implies that $\sigma = n\pi/2$ and $n^- = 0$. Then $q_{\min} = -n/4$ and $q_{\max} = n/4$ and the number of integers in $(-n/4, n/4)$ is $\mathcal{N} = 2 \cdot \mathrm{Int}\left[(n-1)/4\right] + 1$. □

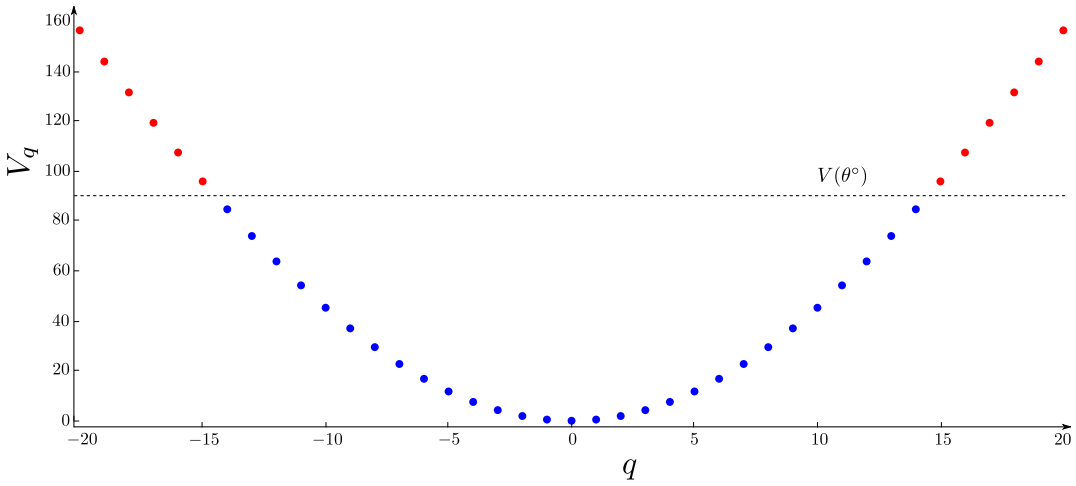

Figure 5: *Value of the LaSalle function V defined in (33) at the stable synchronous states with winding numbers $q \in \{-20, ..., 20\}$, for a directed cycle of length $n = 83$ with coupling strength $a_{i,i+1} = 1$ for all i. If, at initial conditions $\boldsymbol{\theta}^\circ$, the function V takes the value indicated by the dashed black line, then the final winding number corresponds to one of the blue dots, and the red dots cannot be reached.*

Corollary 3.8. *For cycles of length lower than or equal to 4, there is a unique stable synchronous state.*

Remark 3.9. *As in section 2, the results of this section are not subject to any limitation on the magnitude and sign of the coupling strenghts. We thus cover all possible cases of directed cycles with identical natural frequencies.*

3.4 Correlation between initial and final winding numbers

In [27, Theorem 3.4], the authors give some explicit conditions for initial conditions to converge to a given synchronous state. We give here other conditions on initial states limiting the possible final states. The knowledge of stable synchronous states and the LaSalle function V in (33), allow to derive some conditions on the final state of the system, for given initial conditions. We showed that V is monotonically decreasing along the trajectories of the system. Thus, if $V(\boldsymbol{\theta}^\circ) < V(\boldsymbol{\theta}^*)$, starting at $\boldsymbol{\theta}^\circ$, the system cannot converge to the synchronous state $\boldsymbol{\theta}^*$.

For instance, for positive identical coupling constants $a_{i,i+1} \equiv K$, it is known [26] that the stable synchronous states satisfy $\theta_i - \theta_{i+1} = 2\pi q/n$, where $q \in \mathbb{Z}$ is the winding number. At such a state, the function V takes value $V_q := 2nK[1 - \cos(2\pi q/n)]$. Hence, for almost all initial conditions $\boldsymbol{\theta}^\circ$ such that $V(\boldsymbol{\theta}^\circ) \leq V_q$, the system will converge to a stable synchronous state with winding number $|q'| \leq |q|$. This limits the possible final states for given initial conditions (see Figure 5).

These observations suggest that along the time evolution of the system, the winding number tends to decrease. To corroborate this, we simulated the time evolution of (31) for 100 000 random initial conditions, picked with uniform distribution on the state space. We consider a directed cycle of $n = 83$ oscillators, with identical natural frequencies, and for each simulation, we compare the initial and final winding numbers, q_{ini} and q_{fin} respectively. In Figure 6(a), the cloud of points follows a line through the origin with slope larger than one. This implies that even if in some cases, the winding number increases along the simulation, there is a general trend towards a decrease of the winding number along the trajectory of the system, especially for large winding numbers. Figure 6(b) displays, for each values of q_{ini}, the distribution of q_{fin} normalized to zero mean. To the eye, these curves look Gaussian, with identical variance. We then fit a Gaussian distribution to each of them and show their parameters in Figure 6(c). The slope of the mean μ is less than one. This indicates again that winding numbers tend to decrease (in absolute value) along simulations. It is striking to see that the variance is almost the same for all initial winding numbers. We are not able yet to give further insight to this fact.

4 Combination of cyclic and acyclic networks

Based on the results of the previous sections, we extend now our results to networks built with directed cycles and acyclic directed graphs. Given a directed graph $\mathcal{G}_1$, we say that a subgraph $\mathcal{G}_2$ is a *leading component* if there are no edges going out of $\mathcal{G}_2$.

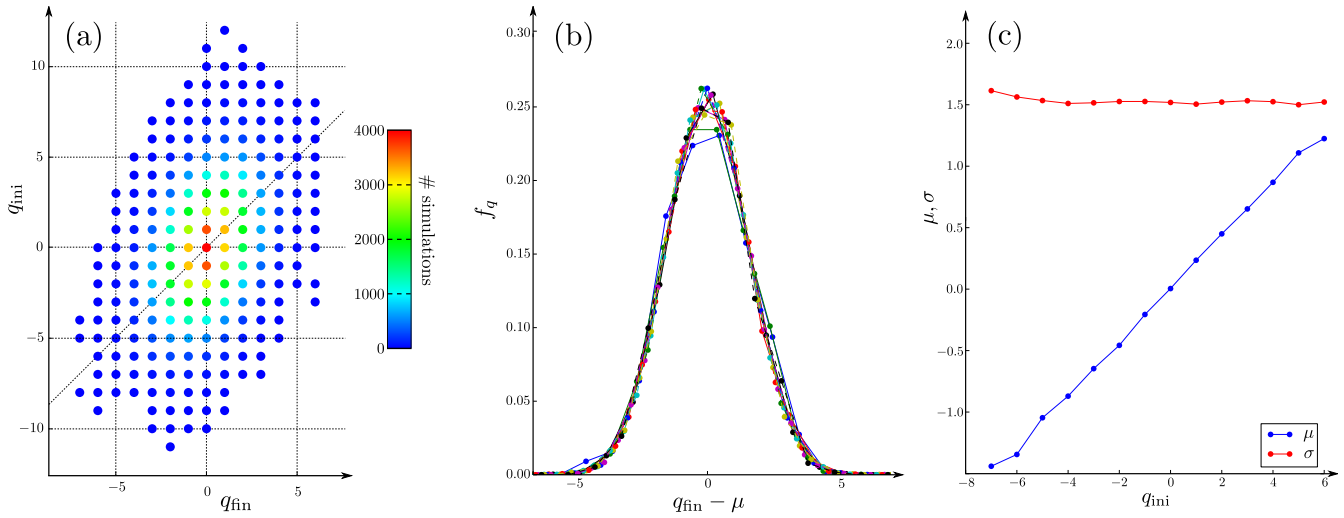

Figure 6: *Panel (a): Distribution of initial and final winding numbers for 100 000 simulations of (31) with* $n = 83$, $\omega_i \equiv 0$ *and random initial conditions. The color code indicates how many simulations started with winding number* q_{ini} *and ended at winding number* q_{fin}. *We see that along simulations, winding numbers tend to decrease in absolute value. For instance, we see that* $|q_{\text{fin}}| < |q_{\text{ini}}|$ *for all simulations with* $|q_{\text{ini}}| > 8$. *Panel (b): Distribution of final winding number for our simulations. Each curve corresponds to a different initial winding number* q_{ini}, *ranging from* -7 *to* 6. *We consider only initial winding number with large enough statistics. For each curve, the mean is normalized to zero. To the eye, each curve follows a similar bell shape. Panel (c): Mean and variance of the Gaussian fit for each curve of panel (b). The slope of the mean with respect to* q_{ini} *is approximately* 0.21, *corroborating the fact that the winding number tends to decrease along simulations.*

4.1 Cases where global synchronization is achieved

4.1.1 One large leading cycle

Consider a graph composed of an acyclic directed graph with a single leading component which is a directed cycle (left panel of Figure 7), whose oscillators have identical natural frequencies. The cycle synchronizes by Theorem 3.1, at a synchronization frequency ω_{s}. The acyclic part is then led by oscillators with identical frequencies. Applying the same recursive argument as in the proof of Theorem 2.1, we can show that all the acyclic part synchronizes, provided that natural frequencies of its oscillators satisfy

$$|\omega_i - \omega_{\text{s}}| \leq \rho_i \,, \qquad\qquad i \in \{1, ..., n\} \,. \tag{55}$$

4.1.2 Multiple small leading cycles

Consider a graph composed of an acyclic directed graph whose leading components are either simple leaders or a leading cycles of length at most 4 (right panel of Figure 7). Here the leaders and the oscillators of the leading cycles have identical natural frequencies. The conditions for global synchronization are then the same as in Theorem 2.1. A cycle of length less than or equal to 4 synchronizes to the frequency of its oscillators because it is too short to carry a nonzero winding number, see Corollary 3.8. The acyclic part is then led by oscillators with identical frequencies and synchronizes following the same recursive argument as in the proof of Theorem 2.1.

4.2 Cases where global synchronization is not achieved

4.2.1 Multiple large leading cycle

A graph composed of an acyclic directed graph with at least two leading components, where (at least) one of them is a leading cycle of length 5 or more (left panel of Figure 8). The leading cycle can synchronize to various frequencies. If it does not synchronizes to the same frequency as the other leader(s), then synchrony cannot be reached. But if it synchronizes to the same frequency, then the network synchronizes. Synchronization is then not global, but is possible for a set of initial conditions with nonzero measure, for some natural frequencies and edge weights.

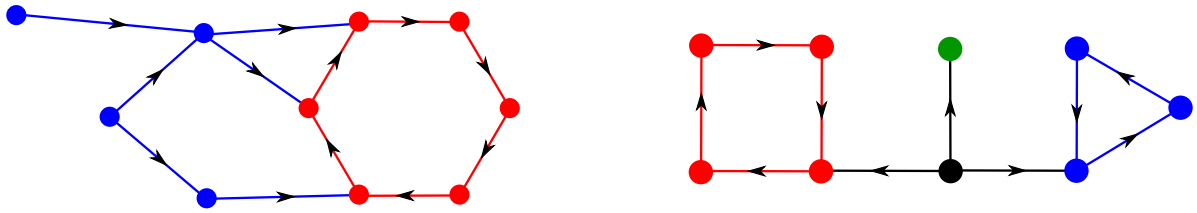

Figure 7: *Left: Example of directed graph with only a leading cycle. The leading cycle is in red and the the blue part is an acyclic directed graph. Such a network globally synchronizes. Right: Example of a globally synchronizing directed graph with multiple leaders and leading cycles of length not larger than* 4.

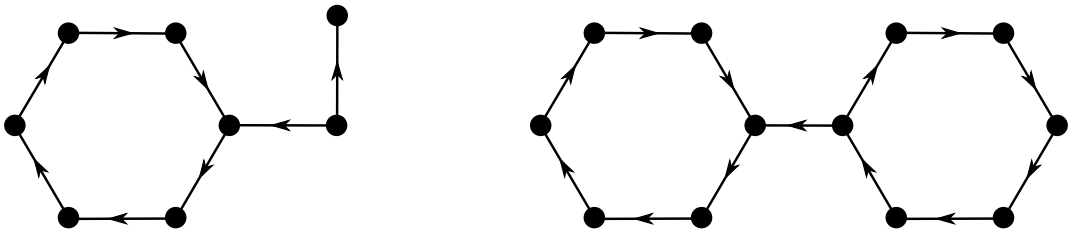

Figure 8: *Left: Example of a nonglobally synchronizing network. The cycle can synchronize to different frequencies depending on the initial conditions and the solitary leader has a fixed frequency. Right: Example of two cycles connected by a directed edge. Simulations indicate that this network does not always synchronize, depending on initial conditions.*

4.2.2 Two large cycles

We numerically verified that two cycles of length more than 5 coupled as in the right panel of Figure 8 can synchronize or not depending on inital conditions. We have not been able to get any analytical insight for this case.

5 Conclusion

We studied the question of synchronization in directed and signed Kuramoto oscillator networks. By considering the simplest directed interaction graphs, we completely characterized frequency-synchronization of the Kurmaoto model on directed and signed acyclic networks and on directed and signed cycles with identical natural frequencies. All our results are valid regardless of the magnitude and sign of the couplings, they are then as general as possible.

In directed and signed acyclic networks, we gave necessary and sufficient conditions for global synchronization and we showed that, if it exists, there is a unique stable synchronous state. We further showed in section 2.2 that, in general, these conditions are as good as they get.

We proved that on directed and signed cycles with identical natural frequencies, the Kuramoto oscillators always synchronizes. Furthermore, we showed that the number of stable synchronous states is finite, and we gave an explicit formula to compute their number. We observed in section 3.4 that, for initial conditions with a given winding number q_{ini}, the distribution of winding numbers after the time evolution of (31) is Gaussian. It is striking that for all values of q_{ini}, the variance of the distribution is identical. We are not able to give any explanation to this fact.

We finally showed through some examples, that in more general directed interaction graphs, the dynamics become much more rich, even for some simple combinations of acyclic graphs and directed cycles.

A Asymptotically autonomous semiflows

In [28], Mischaikow et al. relate the solution of the nonautonomous system $\dot{x} = f(t, x)$ on $\mathbb{R}^n$ to the solution of the autonomous system $\dot{y} = g(y)$ on $\mathbb{R}^n$, where $f(t, \cdot) \to g(\cdot)$ for $t \to \infty$. We give some preliminary definitions and state then two results that we need in the proof of Theorem 2.1.

Definition A.1 (Mischaikow et al. [28]). *Let $\Theta\colon T \times \mathbb{R}^n \to \mathbb{R}^n$ be a continuous function, where $T = \{(t,s)\colon 0 \le s \le t < \infty\}$. The function Θ is a* nonautonomous semiflow *on $\mathbb{R}^n$ if it satisfies*

$$\Theta(s,s,x) = x\,, \qquad s \ge 0\,; \tag{56}$$

$$\Theta(t,s,\Theta(s,r,x)) = \Theta(t,r,x)\,, \qquad t \ge s \ge r \ge 0\,. \tag{57}$$

The semiflow is called autonomous *if in addition*

$$\Theta(t+r,s+r,x) = \Theta(t,r,x)\,. \tag{58}$$

A nonautonomous semiflow Θ is called asymptotically autonomous with limit semiflow Φ*, if Φ is an autonomous semiflow on $\mathbb{R}^n$ and*

$$\Theta(t_j + s_j, s_j, x_j) \ \to \Phi(t,x)\,, \qquad j \to \infty\,, \tag{59}$$

for any sequences $t_j \to t$, $s_j \to \infty$ and $x_j \to x$, with $x, x_j \in \mathbb{R}^n$, $0 \le t, t_j < \infty$, and $s_j \ge 0$.

The ω-limit set *of Θ is*

$$\Lambda_\Theta(s,x_0) \coloneqq \left\{ x \in \mathbb{R}^n\colon \exists\ \{t_j\},\ j \in \mathbb{N},\ \text{s.t.}\ \lim_{j\to\infty} t_j = \infty \text{ and } \lim_{j\to\infty} \Theta(s,t_j,x_0) = x \right\}. \tag{60}$$

Consider the systems of ordinary differential equations $\dot{x} = f(t,x)$ and $\dot{y} = g(y)$ on $\mathbb{R}^n$. Denote by $\Theta(t,s,x_0)$ the solution $x(t)$ of the first system, with $x(s) = x_0$, and denote by $\Phi(t,x_0)$ the solution $y(t)$ of the second system, with $y(0) = x_0$.

Proposition A.2 (Mischaikow et al. [28]). *If $f(t,x) \to g(x)$, $t \to \infty$, uniformly[†] on compact subsets of $\mathbb{R}^n$, then Θ is asymptotically autonomous with limit semiflow Φ.*

Theorem A.3 (Mischaikow et al. [28]). *Let Θ be an asymptotically autonomous semiflow with limit semiflow Φ, and let its orbit $\{\Theta(t,s,x)\colon t \in [0,\infty)\}$ have compact closure in $\mathbb{R}^n$. Then $\Lambda_\Theta(s,x_0)$ is invariant for the semiflow Φ and attracts $\Theta(t,s,x_0)$.*

References

[1] Y. Kuramoto, *Self-entrainment of a population of coupled non-linear oscillators*, in Lecture Notes in Physics, vol. 39. International Symposium on Mathematical Problems in Theoretical Physics, H. Araki, ed., Berlin, 1975, Springer, pp. 420–422, https://doi.org/10.1007/BFb0013365.

[2] S. H. Strogatz, *From Kuramoto to Crawford: exploring the onset of synchronization in populations of coupled oscillators*, Physica D, 143 (2000), pp. 1–20, https://doi.org/10.1016/S0167-2789(00)00094-4.

[3] J. A. Acebrón, L. L. Bonilla, C. J. Pérez Vicente, F. Ritort, and R. Spigler, *The Kuramoto model: A simple paradigm for synchronization phenomena*, Rev. Mod. Phys., 77 (2005), p. 137, https://doi.org/10.1103/RevModPhys.77.137.

[4] F. Dörfler and F. Bullo, *Synchronization in complex networks of phase oscillators: A survey*, Automatica, 50 (2014), pp. 1539–1564, https://doi.org/10.1016/j.automatica.2014.04.012.

[5] G. B. Ermentrout, *The behavior of rings of coupled oscillators*, J. Math. Biol., 22 (1985), pp. 55–74, https://doi.org/10.1007/BF00276558.

[6] J. L. van Hemmen and W. F. Wreszinski, *Lyapunov function for the Kuramoto model of nonlinearly coupled oscillators*, J. Stat. Phys., 72 (1993), p. 145, https://doi.org/10.1007/BF01048044.

[7] J. Buck, *Synchronous rhythmic flashing of fireflies. II.*, Q. Rev. Biol., 63 (1988), pp. 265–289, https://doi.org/10.1086/415929.

[8] G. B. Ermentrout, *An adaptive model for synchrony in the firefly* Pteroptyx malaccae, J. Math. Biol., 29 (1991), pp. 571–585, https://doi.org/10.1007/BF00164052.

[†]Here *uniform* means that $\forall\ \varepsilon > 0$, $\exists\ T > 0$ such that $|f(t,x) - g(x)| < \varepsilon$, $\forall\ t \ge T$ and $\forall\ x \in \mathbb{R}^n$.

[9] Z. Lu, K. Klein-Cardeña, S. Lee, T. M. Antonsen, M. Girvan, and E. Ott, *Resynchronization of circadian oscillators and the east-west asymmetry of jet-lag*, Chaos, 26 (2016), p. 094811, https://doi.org/10.1063/1.4954275.

[10] K. Wiesenfeld, P. Colet, and S. H. Strogatz, *Synchronization transitions in a disordered Josephson series array*, Phys. Rev. Lett., 76 (1996), p. 404, https://doi.org/10.1103/PhysRevLett.76.404.

[11] K. Wiesenfeld, P. Colet, and S. H. Strogatz, *Frequency locking in Josephson arrays: Connection with the Kuramoto model*, Phys. Rev. E, 57 (1998), pp. 1563–1569, https://doi.org/10.1103/PhysRevE.57.1563.

[12] F. Dörfler, M. Chertkov, and F. Bullo, *Synchronization in complex oscillator networks and smart grids*, Proc. Natl. Acad. Sci., 110 (2013), pp. 2005–2010, https://doi.org/10.1073/pnas.1212134110.

[13] E. Mallada and A. Tang, *Synchronization of weakly coupled oscillators: coupling, delay and topology*, J. Phys. A, 46 (2013), p. 505101, https://doi.org/10.1088/1751-8113/46/50/505101.

[14] J. G. Restrepo, E. Ott, and B. R. Hunt, *Onset of synchronization in large networks of coupled oscillators*, Phys. Rev. E, 71 (2005), p. 036151, https://doi.org/10.1103/PhysRevE.71.036151.

[15] D. A. Paley, N. E. Leonard, R. Sepulchre, D. Grunbaum, and J. K. Parrish, *Oscillator models and collective motion*, IEEE Control Syst. Mag., 27 (2007), pp. 89–105, https://doi.org/10.1109/MCS.2007.384123.

[16] R. Sepulchre, D. A. Paley, and N. E. Leonard, *Stabilization of planar collective motion with limited communication*, IEEE Trans. Autom. Control, 53 (2008), pp. 706–719, https://doi.org/10.1109/TAC.2008.919857.

[17] O. Mason and M. Verwoerd, *Graph theory and networks in biology*, IET Syst. Biol., 1 (2007), pp. 89–119, https://doi.org/10.1049/iet-syb:20060038.

[18] C. Börgers and N. Kopell, *Synchronization in networks of excitatory and inhibitory neurons with sparse, random connectivity*, Neural Comput., 15 (2003), pp. 509–538, https://doi.org/10.1162/089976603321192059.

[19] M. T. Schaub, N. O'Clery, Y. N. Billeh, J.-C. Delvenne, R. Lambiotte, and M. Barahona, *Graph partitions and cluster synchronization in networks of oscillators*, Chaos, 26 (2016), p. 094821, https://doi.org/10.1063/1.4961065.

[20] H. Hong and S. H. Strogatz, *Kuramoto model of coupled oscillators with positive and negative coupling parameters: An example of conformist and contrarian oscillators*, Phys. Rev. Lett., 106 (2011), https://doi.org/10.1103/PhysRevLett.106.054102.

[21] O. Burylko, *Competition and bifurcations in phase oscillator networks with positive and negative couplings*, in Proc. of the IEEE NDES, 2012, pp. 1–4.

[22] A. El Ati and E. Panteley, *Asymptotic phase synchronization of Kuramoto model with weighted non-symmetric interconnections: A case study*, in Proc. of the 52nd IEEE CDC, 2013, pp. 1319–1324, https://doi.org/10.1109/CDC.2013.6760065.

[23] A. El Ati and E. Panteley, *Synchronization of phase oscillators with attractive and repulsive interconnections*, in Proc. of the 18th IEEE MMAR, 2013, pp. 22–27, https://doi.org/10.1109/MMAR.2013.6669875.

[24] P. S. Skardal, D. Taylor, and J. Sun, *Optimal synchronization of directed complex networks*, Chaos, 26 (2016), p. 094807, https://doi.org/10.1063/1.4954221.

[25] S.-Y. Ha and Z. Li, *Complete synchronization of Kuramoto oscillators with hierarchical leadership*, Commun. Math. Sci., 12 (2014), pp. 485–508, https://doi.org/10.4310/CMS.2014.v12.n3.a5.

[26] J. A. Rogge and D. Aeyels, *Stability of phase locking in a ring of unidirectionally coupled oscillators*, J. Phys. A, 37 (2004), pp. 11135–11148, https://doi.org/10.1088/0305-4470/37/46/004.

[27] S.-Y. Ha and M.-J. Kang, *On the basin of attractors for the unidirectionally coupled Kuramoto model in a ring*, SIAM J. Appl. Math., 72 (2012), pp. 1549–1574, https://doi.org/10.1137/110829416.

[28] K. Mischaikow, H. Smith, and H. R. Thieme, *Asymptotically autonomous semiflows: Chain recurrence and Lyapunov functions*, Trans. Amer. Math. Soc., 347 (1995), https://doi.org/10.1090/S0002-9947-1995-1290727-7.

[29] R. Potrie and P. Monzón, *Local implications of almost global stability*, Dynam. Syst., 24 (2009), pp. 109–115, https://doi.org/10.1080/14689360802474657.

[30] H. K. Khalil, *Nonlinear systems*, Prentice Hall, 3rd ed., 2002.

[31] R. Delabays, T. Coletta, and P. Jacquod, *Multistability of phase-locking and topological winding numbers in locally coupled Kuramoto models on single-loop networks*, J. Math. Phys., 57 (2016), p. 032701, https://doi.org/10.1063/1.4943296.

[32] J. P. LaSalle and S. Lefschetz, *Stability by Liapunov's Direct Method: With Applications*, vol. 4 of Mathematics in science and engineering, Academic Press, 1961.

[33] D. Manik, M. Timme, and D. Witthaut, *Cycle flows and multistability in oscillatory networks*, Chaos, 27 (2017), p. 083123, https://doi.org/10.1063/1.4994177.

[34] R. A. Horn and C. R. Johnson, *Matrix Analysis*, Cambridge University Press, New York, 1986.

[35] L. G. Khazin and E. E. Shnol, *Stability of Critical Equilibrium States*, Manchester University Press, 1991.